

# Optimal Design of a Rotating Eddy-Current Probe—Application to Characterization of Anisotropic Conductive Materials

Samir Bensaid<sup>1</sup>, Didier Trichet<sup>2</sup>, and Javad Fouladgar<sup>2</sup>

<sup>1</sup>Université de Bouira, Bouïra 10000, Algeria

<sup>2</sup>Institut de Recherche en Energie Electrique de Nantes Atlantique, Saint Nazaire 44600, France

This paper presents the optimal design of a rotating eddy-current probe using the inverse problem method. The probe is dedicated to identify the electrical tensor conductivity of carbon fiber composite materials. A 3-D anisotropic shell elements model associated with annealing optimization algorithm is used to minimize the goal function.

**Index Terms**—Annealing optimization algorithm, composite materials, conductivity measurement, inverse problem, optimal design, sensor phenomena and characterization.

## I. INTRODUCTION

CARBON fiber reinforced composites offer a light-weight high potential material for innovative applications, especially in the aeronautic industry. Their development, however, leads to a higher demand on precise characterization and nondestructive testing methods (NDT). In the case of induction heating or eddy-current NDT, the electrical conductivity is an important physical property to be identified for the carbon fiber reinforced polymers (CFRP) composite materials [1]–[3].

A CFRP composite is an assembly of several layers in which an important number of carbon fibers reinforcements are impregnated in a thermoplastic or thermoset matrix. The fibers orientations are generally different between the layers (Fig. 1). This complex geometry of the composite materials makes very difficult the direct measuring of their electrical conductivity using direct contact ac/dc classical methods.

Contactless eddy-current characterization method using a rotating probe can overcome these difficulties [1]. The availability of high-sensibility eddy-current probes enables the access to a better tensor of electrical conductivity characterization in the different directions.

In this paper, we present the optimal design methodology of a  $U$ -form eddy-current rotating probe to improve the measurement sensibility and the precision of the conductivity tensor evaluation. The inverse problem is used to search the best sizes of  $U$ -form rotating probe. The goal function is constructed on the basis of two criteria as follows.

- 1) To facilitate the resistance measurement of the probe, the minimum resistance must be as high as possible.
- 2) To have the highest sensibility to anisotropy of the material, the probe relative difference resistance between two antagonistic angular positions (positions at high- and low-probe resistances) should be the highest possible.

In our probe optimization (Fig. 2), we have limited the number of optimization parameters to four: the width ( $w_1$ ) and height ( $h_1$ ) of the  $U$ -shape probe; the  $N$ -turns rectangular coil length ( $h_2$ ) and width ( $w_2$ ).

A 3-D anisotropic finite shell elements model associated with simulated annealing algorithm (SAA) is used to minimize

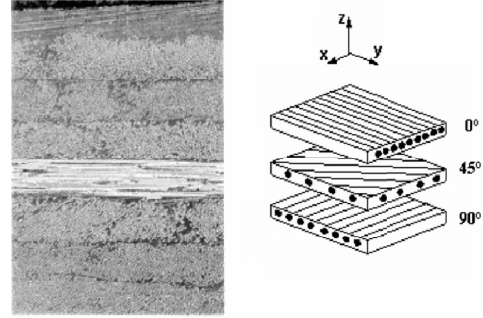


Fig. 1. Anisotropic composite.

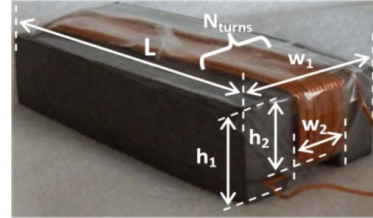


Fig. 2. Rotating  $U$  form probe geometry.

the cost function. SAA is a probabilistic metaheuristic global optimization method [5]–[7].

## II. PROBLEM FORMULATION

The inverse problem optimal design goal function is written as

$$\text{cost} = \frac{R}{\Delta R_{\text{high}} - \Delta R_{\text{low}}} + \frac{R}{\Delta R_{\text{low}}} \quad (1)$$

where  $\Delta R_{\text{high}}$  and  $\Delta R_{\text{low}}$  are, respectively, the highest and the lowest load resistances measured by the probe and  $R$  is a calibration resistance depending on the measuring apparatus.

The resistance variations are computed using the real part of apparent power induced inside the anisotropic shell element [1]

$$\Delta R = \frac{\text{Real}(P)}{I^2} \quad (2)$$

where  $I$  is the source current injected in the probe.

The measured resistance variation is obtained using the precision LCR-meter apparatus at several angular positions of the probe.

Manuscript received May 25, 2014; revised September 11, 2014 and October 3, 2014; accepted October 8, 2014. Date of current version April 22, 2015. Corresponding author: S. Bensaid (e-mail: bensaid2011@gmail.com).

Color versions of one or more of the figures in this paper are available online at <http://ieeexplore.ieee.org>.

Digital Object Identifier 10.1109/TMAG.2014.2363174

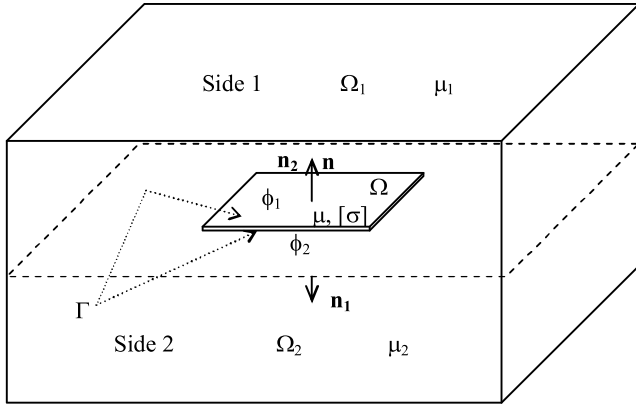


Fig. 3. Eddy-current probe based on rotating magnetic field prototype.

### A. Shell Element Resistance Computation

The apparent power induced in the anisotropic shell element is obtained using the Poynting vector integral [1]–[4]

$$P = \frac{1}{2} \left[ \iint_{S_2} (E_{2s} \times H_{2s}^*) \cdot dS - \iint_{S_1} (E_{1s} \times H_{1s}^*) \cdot dS \right] \quad (3)$$

where  $S_1$  and  $S_2$  are the upper and lower surface areas of the anisotropic shell element.  $\mathbf{E}_{iS}$  and  $\mathbf{H}_{iS}$  are the corresponding electric and magnetic fields on the surface interface with side  $i$  of the solution region (Fig. 3). These neighboring fields are computed using the finite shell element method by following the steps below [4]–[8].

- 1) Write the shell element formulation in side 1

$$\begin{aligned} & \int_{\Omega_1} \mu_1 \text{grad } w \cdot \text{grad } \phi_1 \, d\Omega_1 \\ & + \frac{1}{j\omega} \int_{\Gamma} \text{grad}_s w \cdot [\alpha] \cdot \text{grad}_s \phi_1 \, d\Gamma \\ & - \frac{1}{j\omega} \int_{\Gamma} \text{grad}_s w \cdot [\beta] \cdot \text{grad}_s \phi_2 \, d\Gamma \\ & = \int_{\Gamma} \mu_1 w \cdot H_j \cdot n_1 \, d\Gamma + \frac{1}{j\omega} \int_{\Gamma} \text{grad}_s w \cdot ([\alpha] - [\beta]) \cdot H_j \, d\Gamma \end{aligned} \quad (4)$$

where  $\mathbf{n}_1$  is the normal vector and  $[\alpha]$ ,  $[\beta]$  are the tensors components coefficients depending on the tensor conductivity  $[\sigma]$ . The magnetic permeability of the layer  $\mu$  (CRFP is a nonmagnetic material), the angular frequency of the magnetic field  $\omega$  and the thickness of the composite plate  $e$ .  $\mathbf{H}_{jS}$  is the source field calculated using Biot and Savart's law at the upper and lower surfaces of the shell element. The effect of the eddy current is considered by  $\text{grad } \phi$  in (5).

The expressions of  $[\alpha]$ ,  $[\beta]$  tensors components coefficients are given in Appendix.

- 2) By permuting the indexes 1 and 2 of the normal vector  $\mathbf{n}$ , the reduced scalar potential  $\phi$ , the magnetic permeability  $\mu$ , and the side name  $\Omega$  in (4), obtain the other equation corresponding to the side 2 of the shell [4].
- 3) Solve the equations system to obtain the magnetic scalar potential in the nodes of the mesh. Then, compute the

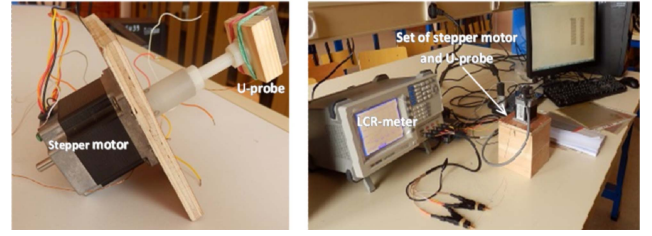


Fig. 4. Shell element representation.

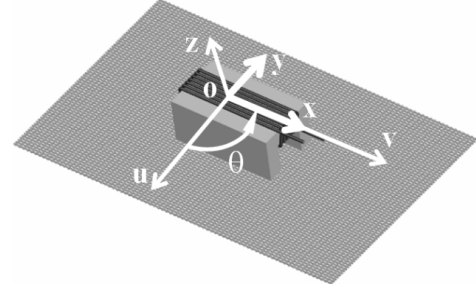


Fig. 5. Rotation angle of the probe.

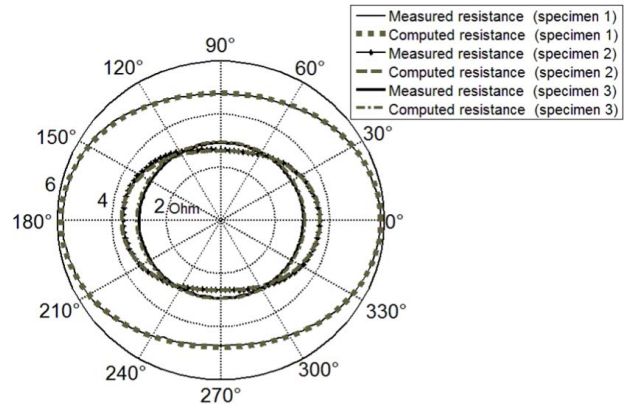


Fig. 6. Measured resistance variations according to angle of some isotropic and anisotropic conductive specimens using the probe demonstration 2.

neighboring magnetic and electric fields

$$\begin{pmatrix} H_{1s} \\ H_{2s} \end{pmatrix} = \begin{pmatrix} H_{js} - \text{grad}_s \phi_1 \\ H_{js} - \text{grad}_s \phi_2 \end{pmatrix} \quad (5)$$

$$\begin{pmatrix} E_{1s} \\ E_{2s} \end{pmatrix} = n_1 \times \begin{pmatrix} -[\alpha] & [\beta] \\ -[\beta] & [\alpha] \end{pmatrix} \begin{pmatrix} H_{1s} \\ H_{2s} \end{pmatrix}. \quad (6)$$

- 4) Calculate the resistance from (2) and (3) at several angular position of the probe for the one layer or the multilayer composite material [9].

### B. Rotating Eddy-Current Probe Prototype

A prototype is realized (Fig. 4) to allow the implementation of the electrical conductivity identification technique for composite anisotropic materials [1].

The system contains the  $U$  probe, a stepper motor, an NI card motor controller, and a precision LCR-meter. All elements of the prototype are controlled by a computer through an NI virtual instrument.

TABLE I  
CHARACTERISTIC OF THE PROBE DIMENSIONS

	L (mm)	$h_1$ (mm)	$h_2$ (mm)	$w_1$ (mm)	$w_2$ (mm)
Probe 1	50	12.7	8.3	35.2	27.4
Probe 2	40	12	9	17	7
Probe 3	40	20	10	31	19

Fig. 6 shows the resistance variation according to the rotating angle of the  $U$  probe (Fig. 5) measured with the performed prototype at frequency of 500 kHz, for three specimens. Specimens 1 and 2 are anisotropic materials and specimen 3 is isotropic one. The  $U$  probe used in this section is dimensioned considering only the anisotropic sensibility criterion and the constraints of ferromagnetic material machining. Characteristic dimensions of the used  $U$  probe demonstration are given in Table I (Probe 2) with a liftoff value of 0.4 mm.

The measurements show clearly that the resistance variation according to the rotating angle of the  $U$  probe has an ellipsoidal shape for the anisotropic materials. On the contrary, for isotropic materials, the shape is circular.

The resistance measurements are also confronted to the computed one using the 3-D anisotropic shell element model and show good concordance for all specimens.

### III. OPTIMIZATION METHOD

In [1], a new approach of the conductivity identification of anisotropic material was presented. It was demonstrated that it is possible to identify the electrical conductivity using a  $U$ -shaped sensor animated with rotational movement. The method has been validated using a well-known anisotropic specimen material. Nelder–Mead’s local minimum research method is used in the inverse model of conductivity identification. This optimization algorithm is limited on the number of optimization parameters.

In this paper, the inverse problem is applied to search the optimal  $U$ -probe dimensions. There are five principal characteristic shaped parameters of the  $U$  probe. The length  $L$ , the width  $w_1$ , and the height  $h_1$  of the probe magnetic circuit, the  $N$  turns rectangular coil length  $h_2$  and width  $w_2$  (Fig. 2). The length  $L$  of the probe is imposed.

To consider such a large number of optimization parameters, SAA is used.

Simulated annealing is a generic probabilistic metaheuristic approach for the global optimization problem of locating a good approximation to the global optimum of a given function in a large search space. It is often used when the search space is discrete.

SAA is inspired by the process of annealing in metallurgy. In this natural process, a material is heated and slowly cooled under controlled conditions to increase the size of the crystals in the material and reduce their defects. The heat increases the energy of the atoms allowing them to move freely, and the slow cooling schedule allows a new low-energy configuration to be discovered and exploited. A new point is randomly generated for all iterations of the SAA. The distance of the new point from the current point, or the extent of the search, is based on a probability distribution with a scale proportional to the temperature. The algorithm accepts all new points that

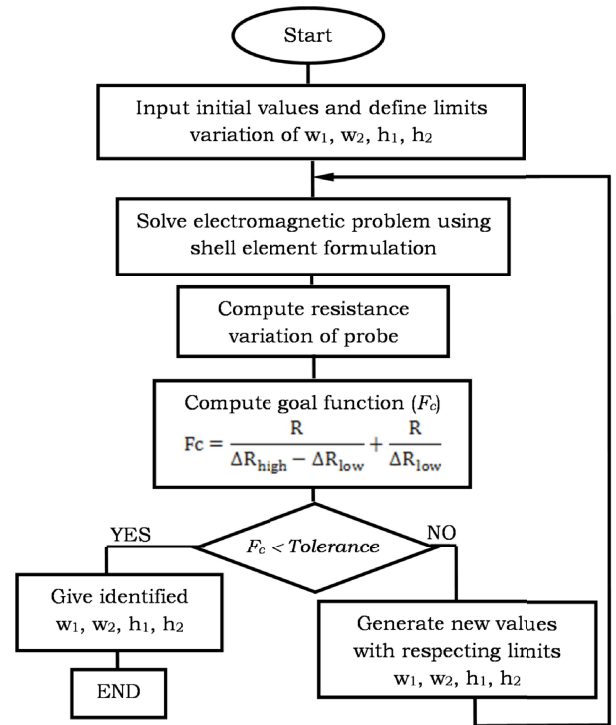


Fig. 7. Design algorithm optimization.

lower the objective, but also, with a certain probability, points that raise the objective. By accepting points that raise the objective, the algorithm avoids being trapped in local minima in early iterations and is able to explore globally for better solutions [5].

The goal function to minimize is given by (1). To have a good precision and a high sensibility in the tensor conductivity identification, the function is constructed by considering two criteria as follows.

- 1) Resistance difference between the two antagonist positions of the probe (positions of low and high variation resistances) must be highest as possible. This criterion allows to clearly distinguishing the lower and higher conductivity of the anisotropic material. It’s the probe sensibility to the low anisotropic.
- 2) The minimum resistance variation of the probe must also be highest as possible. This criterion reduces the measurement uncertainties.

The machining constraints of ferromagnetic material are also considered in the optimization problem.

In the inverse problem (Fig. 7) of seeking the characteristic dimensions of the  $U$  probe, direct problem of resistance computation modeled with shell element is solved for two antagonist angle positions of the probe corresponding to  $\Delta R_{low}$  and  $\Delta R_{high}$ .

### IV. RESULTS AND DISCUSSION

To have the highest precision and the best sensibility of the tensor conductivity identification using the rotating CF probe, the optimal designing of the probe is taken in the low anisotropy situation.

MATLAB programming environment performed with Global Optimization Toolbox is used.

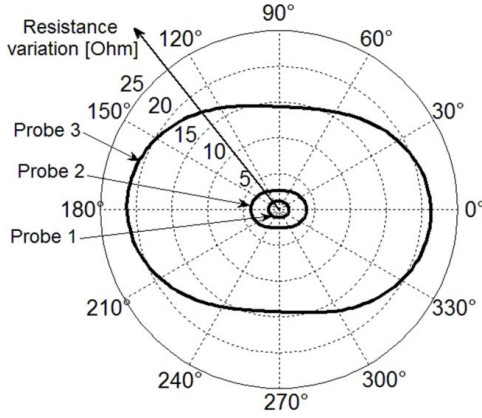


Fig. 8. Computed variation resistance of the designed probe confronted to the probe demonstrations.

The obtained optimal dimensions of the probe are shown in Table I (Probe 3). The imposed liftoff value is 0.4 mm. The turn number of probe is 74.

Fig. 8 shows the resistance variation of the designed probe, at frequency value of 200 kHz. The resistance variation is also compared with two probe demonstrations, the first (probe 1) is the used one in [1] and the second is used for the direct algorithm calibration.

In the simulations, it's assumed that the  $uv$  axis that represents the directions of highest and lowest conductivity of the anisotropic material is a stationary axis. In addition, the  $xy$  axis turns with the same rotation speed of the  $u$ -probe. The considered anisotropic material has the low value of conductivity in  $u$  direction and the high one in  $v$  axis (Fig. 5).

The maximum resistance variation is obtained when the  $U$ -probe axis is oriented in  $u$  direction ( $\theta = 0$ ). The minimum value is obtained when the  $U$ -probe in the  $v$  direction ( $\theta = 90^\circ$ ). The resistance variation of the anisotropic material obtained using the optimized probe (probe 3) is five times better than probe demonstration (probe 1) and 20 times better than the probe demonstration (probe 2).

## V. CONCLUSION

The aim of this paper is the amelioration of the sensitivity and precision in the electrical conductivity identification of anisotropic conductive material. Annealing optimization is used in inverse problem design of the rotation  $U$ -probe. In the direct problem, resistance variation of the probe is computed using 3-D anisotropic shell element simulation model.

The simulation model is validated using an efficient  $U$ -probe for three anisotropic specimen configurations with known conductivity. Then, this validated simulation has been used to design an optimal  $U$ -probe. The  $U$ -probe is designed with considering the resistance difference between two antagonist positions of the probe (positions of low and high variation resistances), the minimum resistance variation of the probe and the machining constraints of ferromagnetic material.

The optimal designed probe allows measuring the tensor components of the electrical conductivity with a better sensitivity and higher precision.

This optimal probe is under construction and will be presented in future works.

## APPENDIX

The  $[\alpha]$  and  $[\beta]$  tensors components coefficients are expressed as follows:

$$[\alpha] = \begin{pmatrix} \alpha_{xx} & \alpha_{xy} \\ \alpha_{yx} & \alpha_{yy} \end{pmatrix} \quad [\beta] = \begin{pmatrix} \beta_{xx} & \beta_{xy} \\ \beta_{yx} & \beta_{yy} \end{pmatrix}$$

$$\begin{cases} \alpha_{xx} = \frac{1}{K_2 - K_1 \cdot \det} \left[ \frac{K_2 P_1}{\tanh(e P_1)} (\sigma_{yx} K_1 + \sigma_{xx}) - \frac{K_1 P_2}{\tanh(e P_2)} (\sigma_{yx} K_2 + \sigma_{xx}) \right] \\ \alpha_{xy} = \frac{1}{K_2 - K_1 \cdot \det} \left[ \frac{P_2}{\tanh(e P_2)} (\sigma_{yx} K_2 + \sigma_{xx}) - \frac{P_1}{\tanh(e P_1)} (\sigma_{yx} K_1 + \sigma_{xx}) \right] \\ \alpha_{yx} = \frac{1}{K_2 - K_1 \cdot \det} \left[ \frac{K_2 P_1}{\tanh(e P_1)} (\sigma_{yy} K_1 + \sigma_{xy}) - \frac{K_1 P_2}{\tanh(e P_2)} (\sigma_{yy} K_2 + \sigma_{xy}) \right] \\ \alpha_{yy} = \frac{1}{K_2 - K_1 \cdot \det} \left[ \frac{P_2}{\tanh(e P_2)} (\sigma_{yy} K_2 + \sigma_{xy}) - \frac{P_1}{\tanh(e P_1)} (\sigma_{yy} K_1 + \sigma_{xy}) \right] \\ \beta_{xx} = \frac{1}{K_2 - K_1 \cdot \det} \left[ \frac{K_2 P_1}{\sinh(e P_1)} (\sigma_{yx} K_1 + \sigma_{xx}) - \frac{K_1 P_2}{\sinh(e P_2)} (\sigma_{yx} K_2 + \sigma_{xx}) \right] \\ \beta_{xy} = \frac{1}{K_2 - K_1 \cdot \det} \left[ \frac{P_2}{\sinh(e P_2)} (\sigma_{yx} K_2 + \sigma_{xx}) - \frac{P_1}{\sinh(e P_1)} (\sigma_{yx} K_1 + \sigma_{xx}) \right] \\ \beta_{yx} = \frac{1}{K_2 - K_1 \cdot \det} \left[ \frac{K_2 P_1}{\sinh(e P_1)} (\sigma_{yy} K_1 + \sigma_{xy}) - \frac{K_1 P_2}{\sinh(e P_2)} (\sigma_{yy} K_2 + \sigma_{xy}) \right] \\ \beta_{yy} = \frac{1}{K_2 - K_1 \cdot \det} \left[ \frac{P_2}{\sinh(e P_2)} (\sigma_{yy} K_2 + \sigma_{xy}) - \frac{P_1}{\sinh(e P_1)} (\sigma_{yy} K_1 + \sigma_{xy}) \right] \end{cases}$$

where

$$K_1 = \frac{\sigma_{yy}}{\sigma_{xy}} - \frac{P_1^2}{j\omega\mu\sigma_{xy}} \quad K_2 = \frac{\sigma_{yy}}{\sigma_{xy}} - \frac{P_2^2}{j\omega\mu\sigma_{xy}}$$

$$P_1 = \sqrt{\frac{j\omega\mu}{2} \left[ (\sigma_{xx} + \sigma_{yy}) + \sqrt{(\sigma_{xx} - \sigma_{yy})^2 + 4 \cdot \sigma_{xy}^2} \right]}$$

$$P_2 = \sqrt{\frac{j\omega\mu}{2} \left[ (\sigma_{xx} + \sigma_{yy}) - \sqrt{(\sigma_{xx} - \sigma_{yy})^2 + 4 \cdot \sigma_{xy}^2} \right]}$$

$$\sigma_{xx} = \sigma_u (\cos \theta)^2 + \sigma_v (\sin \theta)^2$$

$$\sigma_{yy} = \sigma_u (\sin \theta)^2 + \sigma_v (\cos \theta)^2$$

$$\sigma_{xy} = \sigma_{yx} = (\sigma_v - \sigma_u) \cos \theta \sin \theta$$

where  $\sigma_u$  and  $\sigma_v$  are the conductivity components of the composite layer in the direction  $v$  of the fibers and in the direction  $u$  perpendicular to the fibers.

## REFERENCES

- [1] S. Bensaid, D. Trichet, and J. Fouladgar, "Electrical conductivity identification of composite materials using a 3-D anisotropic shell element model," *IEEE Trans. Magn.*, vol. 45, no. 3, pp. 1859–1862, Mar. 2009.
- [2] W. Yin, P. J. Withers, U. Sharma, and A. J. Peyton, "Noncontact characterization of carbon-fiber-reinforced plastics using multifrequency eddy current sensors," *IEEE Trans. Instrum. Meas.*, vol. 58, no. 3, pp. 738–743, Mar. 2009.
- [3] G. Mook, R. Lange, and O. Koeser, "Non-destructive characterisation of carbon-fibre-reinforced plastics by means of eddy-currents," *Compos. Sci. Technol.*, vol. 61, no. 6, pp. 865–873, 2000.
- [4] S. Bensaid, D. Trichet, and J. Fouladgar, "3-D simulation of induction heating of anisotropic composite materials," *IEEE Trans. Magn.*, vol. 41, no. 5, pp. 1568–1571, May 2005.
- [5] R. A. Rutenbar, "Simulated annealing algorithms: An overview," *IEEE Circuits Devices Mag.*, vol. 5, no. 1, pp. 19–26, Jan. 1989.
- [6] Ł. Dowhań, A. Wymysłowski, and K. Urbanski, "Simulated annealing as a global optimization algorithm used in numerical prototyping of electronic packaging," in *Proc. 10th IEEE Int. Conf. T2MPSE2M*, Apr. 2009, pp. 1–5.
- [7] D. Fodorean, L. Idoumghar, A. N'Diaye, D. Bouquain, and A. Miraoui, "Simulated annealing algorithm for the optimisation of an electrical machine," *IET Electr. Power Appl.*, vol. 6, no. 9, pp. 735–742, Nov. 2012.
- [8] C. Guerin and G. Meunier, "3-D magnetic scalar potential finite element formulation for conducting shells coupled with an external circuit," *IEEE Trans. Magn.*, vol. 48, no. 2, pp. 323–326, Feb. 2012.
- [9] S. Bensaid, D. Trichet, and J. Fouladgar, "Electromagnetic and thermal behaviors of multilayer anisotropic composite materials," *IEEE Trans. Magn.*, vol. 42, no. 4, pp. 995–998, Apr. 2006.